Structure of Protein Phosphatase Methyltransferase 1 (PPM1), a Leucine Carboxyl Methyltransferase Involved in the Regulation of Protein Phosphatase 2A Activity

Nicolas Leulliot, Sophie Quevillon-Cheruel, Isabelle Sorel, Ines Li de La Sierra-Gallay, Bruno Collinet, Marc Graille, Karine Blondeau, Nabila Bettache, Anne Poupon, Joël Janin, et al.

▶ **To cite this version:**

Nicolas Leulliot, Sophie Quevillon-Cheruel, Isabelle Sorel, Ines Li de La Sierra-Gallay, Bruno Collinet, et al.. Structure of Protein Phosphatase Methyltransferase 1 (PPM1), a Leucine Carboxyl Methyltransferase Involved in the Regulation of Protein Phosphatase 2A Activity. Journal of Biological Chemistry, 2003, 279, pp.8351 - 8358. 10.1074/jbc.m311484200 . hal-03299364

HAL Id: hal-03299364
https://hal.science/hal-03299364

Submitted on 26 Jul 2021

HAL is a multi-disciplinary open access archive for the deposit and dissemination of scientific research documents, whether they are published or not. The documents may come from teaching and research institutions in France or abroad, or from public or private research centers.

L'archive ouverte pluridisciplinaire **HAL**, est destinée au dépôt et à la diffusion de documents scientifiques de niveau recherche, publiés ou non, émanant des établissements d'enseignement et de recherche français ou étrangers, des laboratoires publics ou privés.

THE JOURNAL OF BIOLOGICAL CHEMISTRY
Vol. 279, No. 9, Issue of February 27, pp. 8351–8358, 2004
© 2004 by The American Society for Biochemistry and Molecular Biology, Inc.
Printed in U.S.A.

Structure of Protein Phosphatase Methyltransferase 1 (PPM1), a Leucine Carboxyl Methyltransferase Involved in the Regulation of Protein Phosphatase 2A Activity*

Received for publication, October 20, 2003, and in revised form, December 2, 2003
Published, JBC Papers in Press, December 4, 2003, DOI 10.1074/jbc.M311484200

Nicolas Leulliot‡§, Sophie Quevillon-Cheruel‡§, Isabelle Sorel‡, Ines Li de La Sierra-Gallay¶, Bruno Collinet‡, Marc Graille¶, Karine Blondeau‖, Nabila Bettache‖, Anne Poupon¶, Joël Janin¶, and Herman van Tilbeurgh‡¶**

From the ‡Institut de Biochimie et de Biophysique Moléculaire et Cellulaire (CNRS-UMR 8619), Université Paris-Sud, Bât. 430, 91405 Orsay, France, the ¶Laboratoire d'Enzymologie et Biochimie Structurales (CNRS-UPR 9063), Bât. 34, 1 Avenue de la Terrasse, 91198 Gif sur Yvette, France, and the ‖Institut de Génétique et Microbiologie (CNRS-UMR 8621), Université Paris-Sud, Bât. 360, 91405 Orsay, France

The important role of the serine/threonine protein phosphatase 2A (PP2A) in various cellular processes requires a precise and dynamic regulation of PP2A activity, localization, and substrate specificity. The regulation of the function of PP2A involves the reversible methylation of the COOH group of the C-terminal leucine of the catalytic subunit, which, in turn, controls the enzyme's heteromultimeric composition and confers different protein recognition and substrate specificity. We have determined the structure of PPM1, the yeast methyltransferase responsible for methylation of PP2A. The structure of PPM1 reveals a common *S*-adenosyl-L-methionine-dependent methyltransferase fold, with several insertions conferring the specific function and substrate recognition. The complexes with the *S*-adenosyl-L-methionine methyl donor and the *S*-adenosyl-L-homocysteine product and inhibitor unambiguously revealed the co-substrate binding site and provided a convincing hypothesis for the PP2A C-terminal peptide binding site. The structure of PPM1 in a second crystal form provides clues to the dynamic nature of the PPM1/PP2A interaction.

The regulation of the serine/threonine protein phosphatase 2A (PP2A),[1] one of the most abundant protein phosphatases in eukaryotic cells, is intimately linked to the ability to modulate the composition of this multimeric enzyme (1). Although several factors such as natural small molecule substrates, other interacting proteins, and reversible phosphorylation have been implicated in the regulation of PP2A function, reversible methylation appears to be central to the regulation of PP2A assembly. Reversible methylation, like phosphorylation, is now appearing to be a fundamental process for the regulation of many cellular processes (2).

Methylation of the mammalian PP2A has been shown to be carried out by a specific methyltransferase (leucine carboxyl methyltransferase 1, also known as LCMT1) (3). Two homologues have been found in *Saccharomyces cerevisiae,* PPM1 and PPM2, which share, respectively, 30 and 26% sequence identity to the mammalian PP2A methyltransferase. It was subsequently shown that only PPM1 was responsible for the methylation of PP2A (4, 5). PPM1 codes for a 37-kDa protein that bears an AdoMet signature sequence motif but, overall, has weak sequence similarities to other methyltransferases. PP2A exists as a heterodimeric or heterotrimeric assembly containing A, B, or C subunits, and the methylation of PP2A occurs on the carboxyl moiety of the C-terminal leucine of the C subunit. The C subunit is the catalytically active component of the enzyme, whereas the A subunit purely acts as a scaffold for the C and B subunits (6). The A subunit first recruits the C catalytic subunit to form the core dimer. The B regulatory subunit comprises (at least) four families, each family containing several isoforms that can bind the AC dimer in a mutually exclusive manner and modulate the PP2A holoenzyme's substrate specificity, enzymatic activity, and/or cellular localization. PP2A is therefore present under various enzymatic species (1). C subunits are well conserved, with ~70% sequence identity across different species. The six C-terminal residues (TPDYFL) are absolutely conserved in all known PP2A C subunits, and the three C-terminal residues (YFL) are also conserved in protein serine/threonine phosphatase PP4 and PP6, suggesting a role for these residues in protein phosphatase regulation.

Methylation of PP2A has been shown to influence the affinity of the AC core dimer for the different B subunits (7, 8). The regulation mechanism seems quite subtle, as some B regulatory subunits appear to bind more efficiently to an AC dimer when the catalytic C subunit has been methylated, whereas other protein partners are not influenced by the C subunit methylation state. The association of the AC core dimer with the regulatory B subunit is governed by equilibrium thermodynamics, and the methylated state of the C subunit is itself in equilibrium between the opposing actions of PPM1 and PPE1, the corresponding methylesterase responsible for removal of the methyl group of PP2A. Variation of the ratios of methyltransferase and methylesterase proteins or modulation of the activity of these two enzymes is therefore a dynamic method

* This work is supported by grants from the Ministère de la Recherche et de la Technologie (Programme Génopoles) and the Association pour la Recherche contre le Cancer (to M. G.). The costs of publication of this article were defrayed in part by the payment of page charges. This article must therefore be hereby marked "*advertisement*" in accordance with 18 U.S.C. Section 1734 solely to indicate this fact.

The atomic coordinates and structure factors (code 1RJD, 1RJE, 1RJF, and 1RJG) have been deposited in the Protein Data Bank, Research Collaboratory for Structural Bioinformatics, Rutgers University, New Brunswick, NJ (http://www.rcsb.org/).

§ These authors contributed equally to this work.

** To whom correspondence should be addressed. E-mail: herman@lebs.cnrs-gif.fr.

[1] The abbreviations used are: PP2A, protein phosphatase 2A; PPM, protein phosphatase methyltransferase; AdoHCys, *S*-adenosyl-L-homocysteine; SeMet, selenomethionine; PEG, polyethylene glycol; MES, 4-morpholineethanesulfonic acid; MT, methyltransferase.

TABLE I
Crystallographic data

				Crystal form I ($P6_5$)		Crystal form II ($P2_12_12_1$)	
	Peak	Edge	Remote	AdoMet	AdoHCys	Apo	AdoHCys
Wavelength (Å)	0.97888	0.97966	0.97243	0.94	0.93	0.98	1.54
Unit-cell parameters *a*, *b*, *c* (Å)	111.3, 111.3, 162.7			110.7, 110.7, 165.9	110.7, 110.7, 165.6	112.4, 112.4, 162.85	47.4, 76, 84.5
Resolution (Å)	30.8–1.97			52–1.80	24–2	30–2.25	56.8–1.87
Total number of reflections	558,140	555,560	398,735	631,127	294,159	290,033	71,628
Total of unique reflections	77,990	78,118	79,683	106,254	76,511	53,908	21,568
Multiplicity	7.2	7.1	5	5.9	3.8	5.4	3.3
R_{merge}[a]	0.07	0.08	0.07	0.13	0.12	0.07	0.09
$I/\sigma(I)$	6.8	5.5	6.3	4.2	5.7	9.1	6
Overall completeness (%)	97.2	97.3	97.2	100	98.8	97.6	83.2
FoM[b] (after DM)	0.5 (0.66)						
Refinement							
Reflections (working/test)				100,754/5,424	72,598/3,851	51,135/2,739	20,438/1,109
R_{cryst}/R_{free}[c]				17.2/21.4	15.3/21	18.3/23.9	17.6/26.2
Non-hydrogen atoms				8,878	9,100	8,225	2,606
Water molecules				770	989	272	136
Bonds (Å)				0.005	0.005	0.005	0.005
Angles (°)				0.78	0.79	0.80	0.84
Mean B factor (Å^2) Prot/sol				14	17	36	26
Ramachandran analysis							
Most favored				93.4	88.9	88.7	92.4
Allowed				6.3	10.9	11.2	7.6
Disallowed				0.3	0.1	0.1	0

[a] $R_{merge} = \Sigma_h\Sigma_i|I_{hi} - \langle I_{hi}\rangle|/\Sigma_h\Sigma_i I_{hi}$, where I_{hi} is the ith observation of the reflection h and $\langle I_{hi}\rangle$ is the mean intensity of reflection h.
[b] FoM, figure of merit.
[c] $R_{factor} = \Sigma\|F_o| - |F_c\|/|F_o|$. R_{free} was calculated with a set of randomly selected reflections (5%).

used in the cell for the regulation of PP2A substrate specificity and subcellular localization (9).

PP2A regulates a variety of cellular processes, such as progression through the cell cycle, DNA replication, signal transduction, translation, apoptosis, and stress response (reviewed in Ref. 10–12). The regulation of such a plethora of essential molecular and cellular processes makes PP2A indispensable for eukaryotic cell survival but also means that the disruption of PP2A function is linked to a number of pathologies. PP2A has been involved in the development of cancer in some studies and described as a tumor suppressor in others (13). Different PP2A assemblies can therefore assume the regulation of opposing functions such as stimulating or inhibiting cell growth, necessitating a dynamic and precise regulation of PP2A function and assembly in the cell.

Recently, a central role for the methylation of PP2A has been suggested in the pathogenesis of Alzheimer's disease caused by elevated homocysteine concentration in the cell (14). Indeed, PP2A is essential for efficient dephosphorylation of the tau protein, and hyperphosphorylation of tau is involved in the development of this disease. Methylation of the AC dimer increases the affinity for the Bα subunit, which directs PP2A activity toward tau. Homocysteine converts to AdoHCys in the cell, and, because AdoHCys is an inhibitor of methyltransferases, this leads to a decrease of PP2A methylation, providing a link with the disease.

In an effort to understand the factors affecting the methylation of PP2A at the molecular level, we have determined, by x-ray crystallography, the structure of the yeast PPM1 methyltransferase as well as the structures of complexes with its co-factor (AdoMet) and product (AdoHCys). The analysis of the three structures has enabled us identify the plausible PP2A binding site and to propose elements important for the specificity of the interaction between PPM1 and PP2A.

MATERIALS AND METHODS

Cloning, Expression, and Purification—The *YDR435c* gene was amplified by PCR (from a sequenced S288C genomic template DNA) and cloned in a modified pET9 vector with an addition of six histidine codons at the 3′-extremity. The transformed Xl-10 Gold expression strain (Stratagene) was grown in 2× YT medium (BIO101 Inc.) at 37 °C up to an $A_{600\ nm}$ of 1. Expression was induced with 0.3 mM isopropyl-1-thio-β-D-galactopyranoside, and the cells were grown for a further 4 h at the same temperature. Cells were collected by centrifugation, resuspended in 20 mM Tris-HCl, pH 8, 200 mM NaCl, and 5 mM β-mercaptoethanol, and stored at −20 °C. Cells were lysed by two cycles of freeze/thawing and sonication and were then centrifuged at 13,000 × *g*. The His-tagged protein was purified using a Ni^{2+} affinity column (Qiagen Inc.) and standard protocols. Eluted protein was further purified by gel filtration using a Superdex™ 75 (Amersham Biosciences) equilibrated against 20 mM Tris-HCl, pH 8, 200 mM NaCl, and 10 mM β-mercaptoethanol. The purity and integrity of the protein was checked by SDS-PAGE and mass spectrometry. SeMet-labeled protein was prepared as described (15, 16) and purified as the native protein.

Crystallization and Data Collection—The protein (3 mg/ml) was crystallized at 293 K by the hanging drop vapor diffusion method from 1:1 microliter drops of protein and precipitant. Two different crystal forms were obtained. Crystal form I of the native protein grew from a mother liquor containing 15% PEG 8000 and 0.1 M KPO_4 or $NaPO_4$, pH 4.6. Crystal form I of the ligand-bound PPM1 was obtained with either 5 mM AdoMet or 5 mM AdoHCys added to the protein solution and mother liquor containing 15% PEG 8000, 0.2 M ammonium sulfate, and 0.1 M MES, pH 5.6. A SeMet-labeled protein in complex with AdoMet was crystallized in 20% PEG 8000, 0.1 M sodium acetate, and 0.1 M MES, pH 5.6. All these conditions yielded rod-like crystals. Crystal form II of the PPM1/AdoHCys complex was obtained in 24% PEG 4000, 0.2 M magnesium chloride, and 0.1 M Tris-HCl, pH 8.5. All crystals were transferred to a cryoprotecting solution composed of the mother liquor and 30% glycerol prior to flash freezing in liquid nitrogen.

X-ray diffraction data on the native PPM1, the native PPM1-AdoMet complex, and the SeMet-substituted protein in complex with AdoMet were collected on the BM30-FIP beamline at the European Synchrotron Radiation Facility. The native PPM1/AdoHCys complex was recorded on the ID14-4 beamline, and the crystal form II of the PPM1/AdoHCys complex was recorded on a Rigaku rotating anode. Data were processed using MOSFLM and SCALA (17). The form I crystals belong to the $P6_5$ space group with three molecules per asymmetric unit, and crystal form II belongs to the $P2_12_12_1$ space group with one molecule per asymmetric unit. The cell parameters and data collection statistics are reported in Table I.

Structure Solution and Refinement—The structure was solved by multiwavelength anomalous diffraction (MAD) using data collected at three wavelengths on the PPM1-AdoMet complex in crystal form I at a resolution of 1.97 Å. The SOLVE (18) program retrieved 24 of 36 possible SeMet sites using the entire resolution range, yielding an interpretable electronic density map. Solvent flattening was performed by RESOLVE (18), and the quality of the map allowed for 90% of the residues to be built automatically. After preliminary rebuilding cycles, the model was fully refined and completed from the high resolution

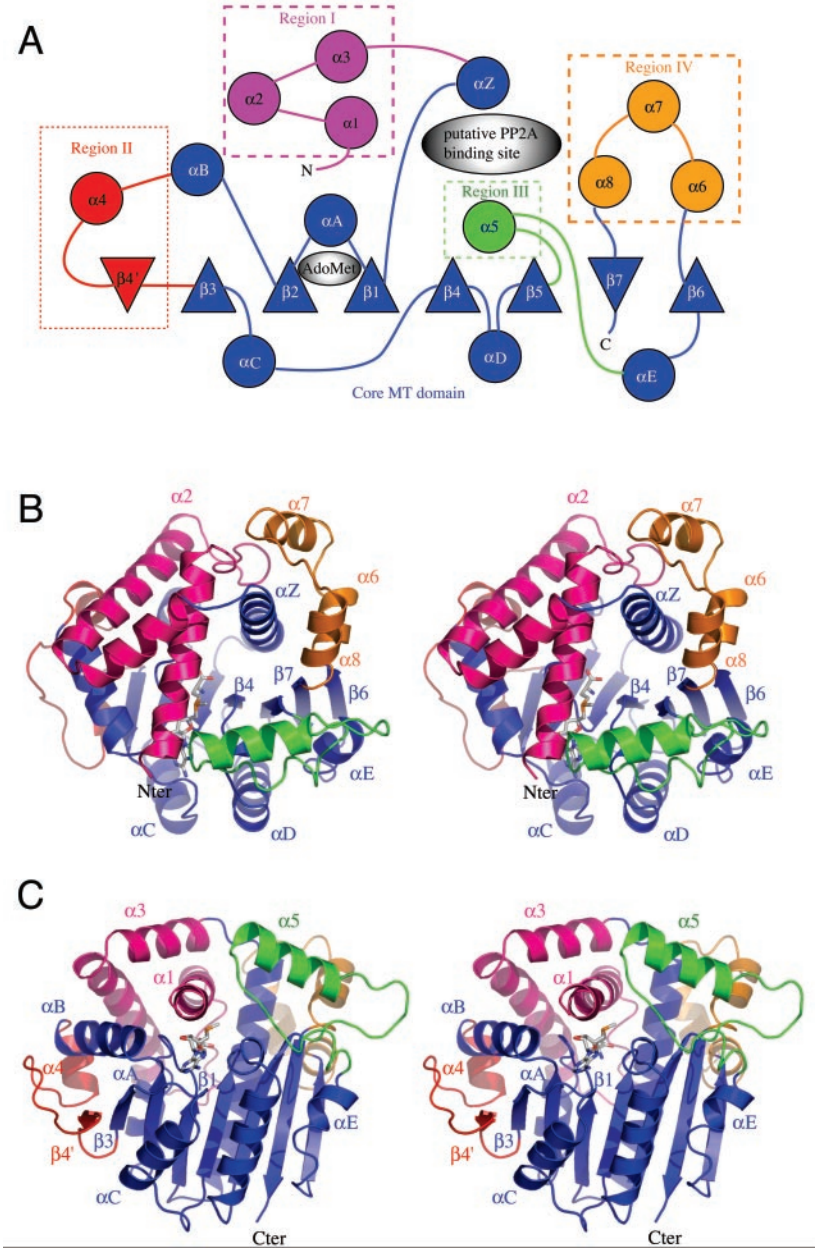

FIG. 1. **Structure of the PPM1 methyltransferase.** *A*, topology diagram of the PPM1 methyltransferase (31). The different domains not belonging to the core methyltransferase fold are *boxed*. The plane of the core β-sheet is perpendicular to the plane of the figure, and the core α-helices are roughly parallel to the strands of the β-sheet. The binding site for AdoMet (or AdoHCys) and the putative binding site for the C-terminal peptide of PP2A are indicated. The secondary structure elements are color-coded as follows: *blue*, core MT domain; *pink*, region I; *red*, region II; *green*, region III; and *orange*, region IV. *B* and *C*, stereo ribbon representation of the structure of PPM1 in crystal form I bound to AdoMet (*stick*). The same color code as in *panel A* is used. Only some of the secondary structure elements are labeled for clarity. No significant conformational rearrangements are observed between the AdoMet, AdoHCys, or apoprotein structures. In crystal form II, the α helix of region III could not be seen in the electron density map and is missing from the model. Structure views are generated using PyMol (pymol.sourceforge.net/). The view in *panel C* is 90° rotated compared with that in *panel B*. *Nter*, N terminus; *Cter*, C terminus.

native data recorded on the PPM1-AdoMet complex using REFMAC and O (17, 19). Structures of the apoprotein and AdoHCys complex in crystal form I were solved directly by transferring the model using one step of rigid body refinement followed by refinement and rebuilding. The structure of PPM1 in the crystal form II was solved by molecular replacement using the AMORE program (20) with a single molecule from the crystal form I as a search model. Refinement statistics are shown in Table I.

The final models in the crystal form I contain residues 2–330, and four residues belonging to the C-terminal His-tag could also be modeled in one monomer. In crystal form II, the model contains residues 8–331, but no electron density could be observed for residues 236–258, and this part of the protein is therefore missing from the model. Two cysteine residues (Cys-15 and Cys-202) were found to be reduced with β-mercaptoethanol in all proteins.

RESULTS AND DISCUSSION

Overall Structure of PPM1—The topology of PPM1 is shown in Fig. 1 along with a stereo ribbon representation from two perpendicular views. The overall structure of PPM1 shows a central β-sheet with several α-helices packing on both sides. A search for structural homologues with the Dali server (www.ebi.ac.uk/dali/) revealed structural similarity with various methyltransferases that act on a wide range of substrates as diverse as small molecules, nucleic acids, and proteins. However, the structural similarity of PPM1 with the other methyltransferases is limited to a central protein core domain common to the class I AdoMet-dependent methyltransferases (*blue domain* in Fig. 1) (21, 22). Fig. 2 shows the superposition of the core AdoMet-dependent methyltransferase domain of PPM1 with the backbone trace of the core MTs of five structurally related enzymes, all acting on either proteins or small molecules. It can be seen that the core methyltransferase fold is well conserved, with the α-helices packing in a very similar orientation on the β-sheet. This core MT domain is characterized by alternate α/β secondary structure elements forming a central β sheet containing seven β-strands (β1 to β7) in the order β3, β2, β1, β4, β5, β7, and β6; six are parallel (β3–β5 and β6) and one is anti-parallel (β7). The six α-helices (αZ and αA–αE) are oriented roughly parallel to the β-strands, and the number of α-helices are distributed equally on each side of the β-sheet (23).

In addition to the conserved core MT fold, PPM1 contains

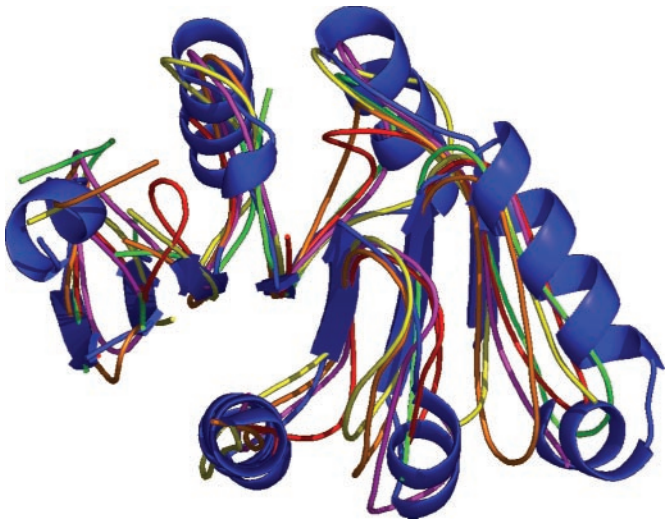

FIG. 2. **Structure conservation of the core MT domain.** The PPM1 core MT domain (in *blue ribbons*) is superimposed with the backbone trace of five other MTs, namely protein L-isoaspartate-*O*-methyltransferase (PDB code 1JG3, *red*), chemotaxis receptor (1BC5, *violet*), phenylethanolamine *N*-methyltransferase (1HNN, *yellow*), glycine *N*-methyltransferase (1XVA, *green*) and Yeco methyltransferase (1IM8, *orange*). Although the core domain of these enzymes is well conserved, their substrates are very diverse. Different substrate specificities are acquired through additions and insertions to the core domain.

several insertions and variations, a commonly used strategy by the members of this enzyme superfamily to confer diverse substrate specificity (23). However, none of these additions and insertions have a similar structural counterpart in any methyltransferase reported to date. These additions to the core domain can be divided in four regions (Fig. 1). Region I consists of three α-helices (α1, α2, and α3) at the N-terminal. The three helices pack on one side of the β-sheet, firmly fixing this subdomain to the core domain. Helix α1 interacts with helix αZ and the loop between β1 and αA. Helix α2 packs in a roughly parallel orientation on helix α1 and on helix αB of the core domain and α4 from region II. Helix α3 packs perpendicularly on helix α1, thereby clamping helix α1 between α2 and αZ. Region II is an insertion between αB and β3. Region II contains an α-helix (α4), followed by a long loop and a strand (β4′) anti-parallel to β3, thereby extending the core β-sheet. Region III is a 33-residue insertion between β5 and αE containing a 12-residue α-helix (α5) that sits on top of the β-sheet. Region IV is a 34-residue insertion between β6 and β7, a common insertion site in MTs. This region contains three α-helices (α6, α7, and α8) that pack against helix αZ through hydrophobic interactions, although α7 makes additional contacts with the loop between α1 and α2, thereby completely burying the C-terminal of helix αZ inside the protein.

Comparison with PP2A MT from Other Organisms—Fig. 3 shows the alignment of the *S. cerevisiae* PPM1 sequence with those of PP2A methyltransferases that have been identified in other organisms, including *Homo sapiens*, *Drosophila melanogaster*, *Caenorhabditis elegans*, *Arabidopsis thaliana*, and *Schizosaccharomyces pombe*, as well as the related *S. cerevisiae* PPM2 and its homologs from *Mus musculus* and *H. sapiens*. The secondary structure of *S. cerevisiae* PPM1 is reported on top of the alignment. As can be expected, most of the core MT domain is conserved, with the best conserved residues located in loops or in the additional regions. One notable exception is helix α1 at the N terminus of region I, whose length and composition vary greatly in each organism and is missing in *S. pombe* and *M. musculus*. The sequence of region I corresponding to helix α2 and α3 in *S. cerevisiae* is also poorly conserved. The position of helix α1, which is almost totally buried inside the protein (Fig. 1*C*), makes it an indispensable element for the structural integrity of region I of PPM1. Removal of this helix would remove hydrophobic contacts with helices α2 and α3, thereby destabilizing the two other helices of this domain. It is therefore likely that the region I in protein phosphatase methyltransferases from different species is structurally different. In addition, region II (helix α4 and β-strand β4′) and, in particular, the large loop between α4 and β4′ seem to be poorly conserved. In crystal form I this loop is involved in intermolecular contacts but, nevertheless, is poorly defined. This is not thought to reflect possible intermolecular interactions occurring *in vivo*, notably with PP2A subunits, which are highly conserved. In contrast to the regions I and II, the sequences of regions III and IV are well conserved. The strictly conserved residues in these regions will be discussed in the context of AdoMet and PP2A binding.

AdoMet Binding Site—The crystal form I has been obtained both in the free form and in the presence of AdoMet and AdoHCys. Examination of the electron density maps during refinement ($2F_o - F_c$ and $F_o - F_c$, with F_o and F_c observed and calculated structure factors, respectively), which were obtained from data collected on the AdoMet and AdoHCys co-crystals, allowed these ligands to be modeled unambiguously in the density. For crystals of the apo form, some residual density in the binding pocket, arising from partial occupancy of some sites by a molecule co-purified from the *Escherichia coli* broth, was detected. The residual density could not be assigned with certainty, probably due to partial occupancy by ligands. Nevertheless, this structure will be called the apo form.

No significant differences are observed between the apo form and the AdoMet or AdoHCys bound complexes or between the three monomers in the asymmetric unit (root mean square deviation is ~0.2 Å for all Cα positions). As illustrated in Figs. 1, 4, and 5, both ligands are bound within a deep pocket at the center of the protein, with contributions from the core MT and from region I. The loop between β1 and αA contains the conserved G*X*G AdoMet binding motif characteristic of class I methyltransferases (23). In PPM1, AdoMet binding follows the same mode as other methyltransferases containing this motif. The adenine base of AdoMet is stabilized by stacking interactions with Tyr-129 and hydrogen bonds between the N6 and N1 positions and the Asp-175 and Asn-177 side chains and the Cys-174 and Leu-176 backbone oxygens. The ribose moiety is fixed by the following: 1) two hydrogen bonds between its O_2' and O3′ hydroxyls and the Asp-128 carboxylate oxygens; and 2) additional hydrophobic contacts with the side chains from Leu-203 and Tyr-206. Electrostatic interactions with Glu-201 and Arg-81 are preponderant with the charged tail of the AdoMet residue (Fig. 4).

Superposition of the AdoMet and AdoHCys PPM1 complexes shows that removal of the methyl group from AdoMet does not influence the conformation of the ligand in the binding pocket (not illustrated). AdoHCys occupies the same site and adopts the same conformation as AdoMet and, therefore, acts as a competitive inhibitor of PPM1. In the AdoHCys bound structure, the electron density clearly shows that the methyl group is replaced by a bound water molecule.

Although the location and general architecture of the AdoMet binding site is well preserved within the MT superfamily, considerable differences exist regarding the exact chemistry of interaction and accessibility of the bound ligand. In PPM1, the binding pocket is lined by residues from the core MT and from helix α1, which forms a cover above the bound ligand. The solvent-exposed surface of AdoMet is 8 Å^2 (as calculated from the program AREAIMOL; Ref. 17), which rep-

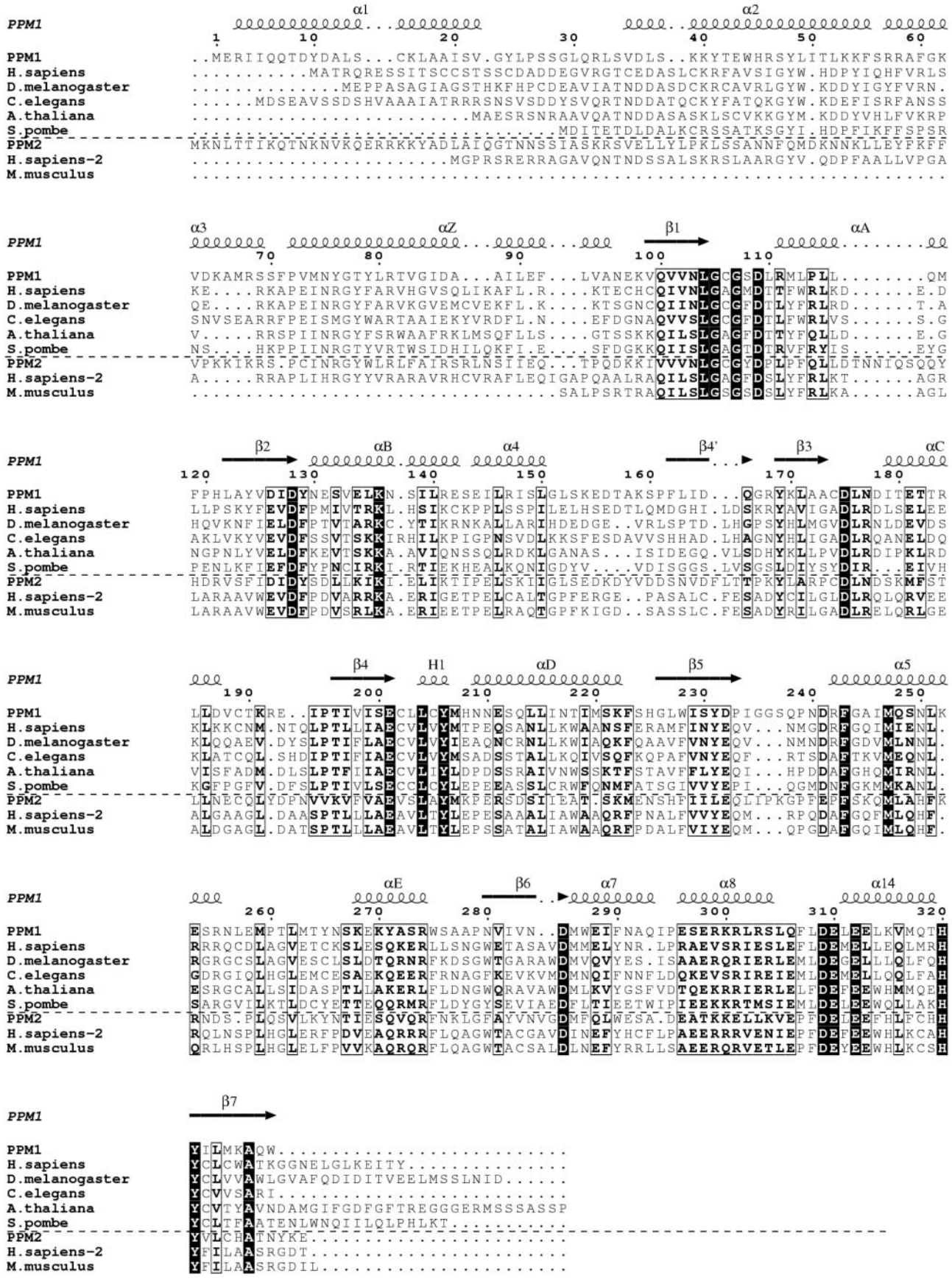

FIG. 3. **Sequence alignment of leucine carboxyl methyltransferases.** Aligned sequences correspond to *S. cerevisiae* PPM1, *H. sapiens* LCM1 (Q9UIC8), *D. melanogaster* (Q9V3K7), *C. elegans* (P46554), *A. thaliana* (Q8VY08), *S. pombe* (O94257), *S. cerevisiae* PPM2 (Q08282), *H. sapiens* (O60294), and *M. musculus* (Q8BYR1) using the program ESPript (32). The PPM1 and PPM2 subfamilies are separated by a *dashed line*. Members of the PPM2 family contain a C-terminal extension of ~300 residues, which has been omitted from the figure. The superposed secondary structure is extracted from the present PPM1 structure.

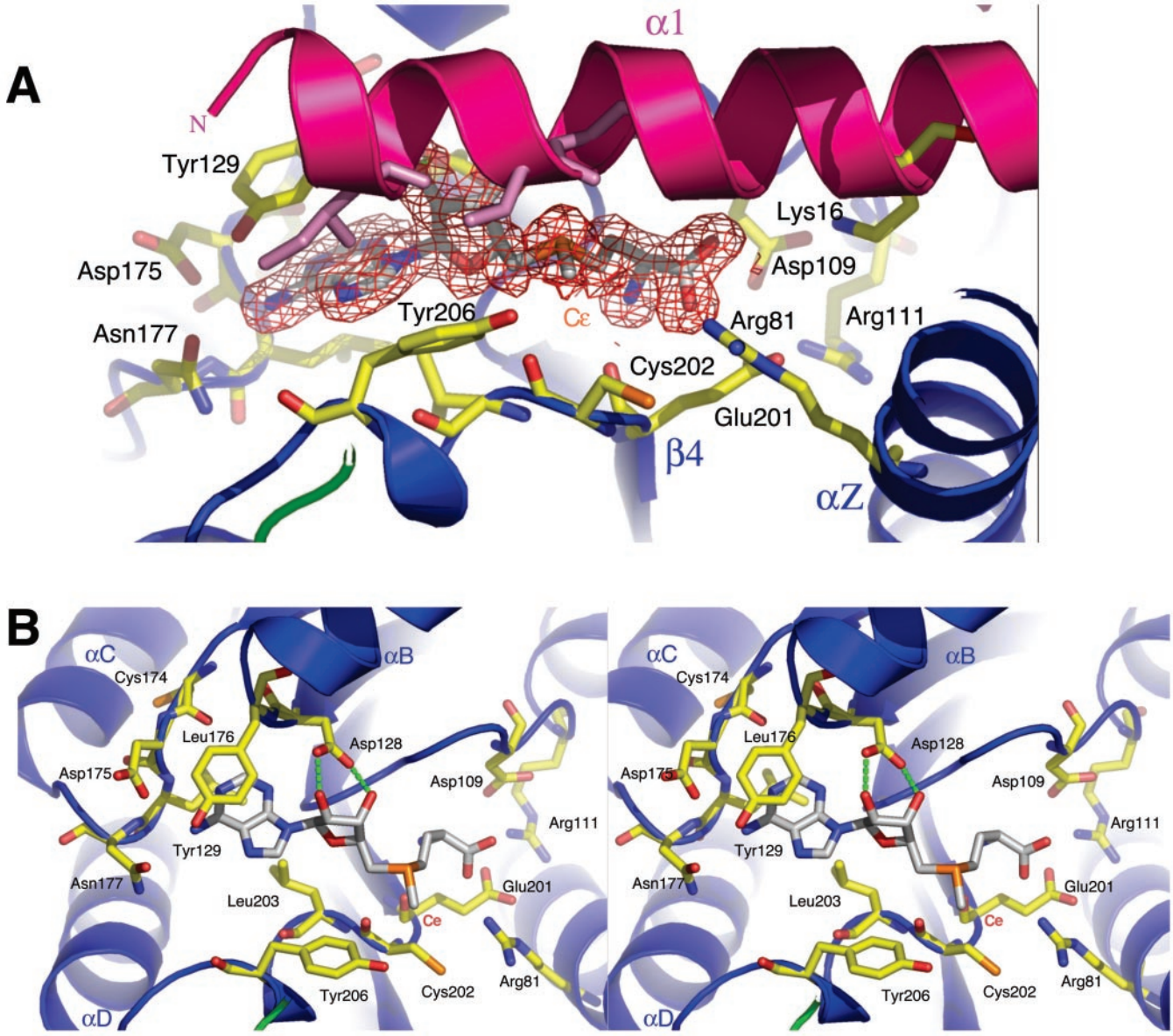

FIG. 4. **AdoMet and PP2A binding sites.** *A*, detailed view of the AdoMet binding site. The $2F_o - F_c$ electronic density (contoured at 1 σ) is represented around the AdoMet cofactor. Residues involved in binding are represented in *sticks*. Helix α1 lies on top of AdoMet and makes mostly nonspecific hydrophobic interactions with AdoMet. No significant changes are observed between the AdoMet and AdoHCys complexes (not shown). *B*, same as *panel A*, rotated >90°. Helix α1 has been omitted to show the more specific interactions of the other residues with AdoMet.

resents 1.3% of the total surface of AdoMet, values that range between 2 and 100 Å^2 in other MTs. The core MT provides all the specific interactions, whereas helix α1 makes mostly nonspecific contacts with AdoMet through Ile-5, Thr-8, and Asp-9. The helix forms a lid above the bound ligand but probably does not contribute to binding specificity (Fig. 4). This could explain why helix α1 is not conserved within the PPM family (see alignment, Fig. 3). Considerable structural variability is observed for the lid regions of MTs in general, which are composed of α-helices, β-strands, or loops.

AdoMet is accessible in the PPM1 complex from two different directions. First, the partially exposed N7 position of the adenine ring of AdoMet defines clearly the entrance of the AdoMet binding cavity. This entrance is occluded by the N terminus of helix α1 and by three loops (β2/αB, β3/αC, and αD/β5). In order for AdoMet to enter or for AdoHCys to exit the binding cavity, a relatively large conformational change in the protein would be necessary. In some MTs, the different conformation of bound AdoMet and AdoHCys is thought to reflect the conformational change that occurs after the catalytic transfer of the methyl group from AdoMet to the substrate (24). This conformational change would help to expel AdoHCys out of the binding site. We have found no crystallographic evidence for conformational flexibility in PPM1; structures obtained in various space groups and enzyme-ligand complexes show identical and well defined binding site conformations. This indicates a rather rigid and stable binding site that requires large conformational changes for substrate binding or for product release, although it does not preclude the existence of an open apoprotein structure in a solution containing a more accessible binding site. In crystal form II, the seven N-terminal residues of helix α1 are disordered and might reflect a flexibility in this region that enables the AdoMet to enter the cavity. It thus appears that binding of the correct cofactor to PPM1 is necessary before binding to the PP2A AC dimer, a conformational rearrangement of PPM1 in the trimeric PPM1 core dimer complex being unlikely.

Protein Phosphatase 2A Binding Site of PPM1—The pre-

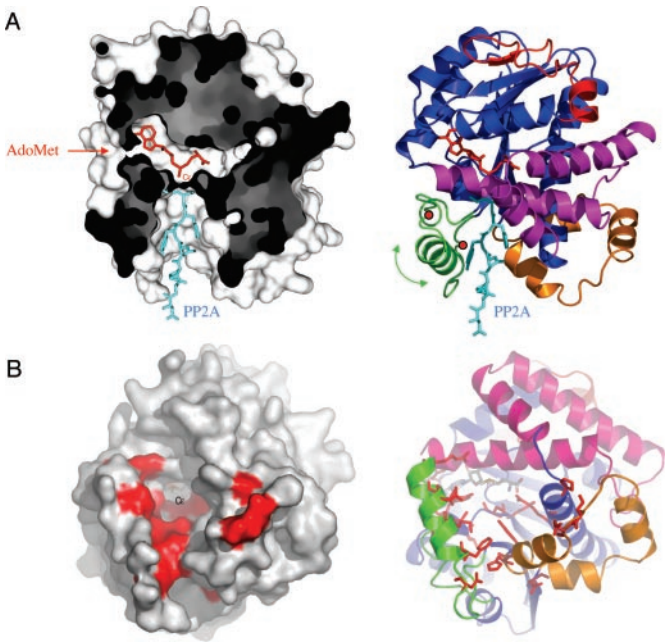

FIG. 5. **Putative PP2A binding site.** *A*, sliced representation of the PPM1 surface (*left*) and the corresponding ribbon representation (*right*). The AdoMet molecule (*red sticks*) is deeply buried inside the protein. A conformational change is necessary for AdoMet to enter or for AdoHCys to exit the cavity. The methyl group is accessible through a second cavity perpendicular to the AdoMet binding cavity, which may constitute the binding site for the PP2A C-terminal acceptor substrate. A model of the six-residue peptide (*light blue*) representing the six C-terminal TPDYFL residues of the PP2A catalytic subunit is shown. The flexibility of helix α5 could enable it to act as a flap over the PP2A binding site. The hinge residues of helix α5 (for which no density is seen in crystal form II) are indicated by *red dots*. *B*, surface (*left*) and corresponding ribbon (*right*) view of the PP2A binding cavity. The Cϵ methyl group is accessible through a small window at the bottom of the cavity. The surface is colored *red* according to the conserved residues in the PPM1 family of Fig. 4. These conserved residues line the interior of the cavity and are therefore probably important for PP2A binding.

ferred substrate of protein phosphatase MTs is the C-terminal leucine of the PP2A catalytic unit. The second access to AdoMet is through a conical cavity ~14 Å deep, penetrating to the center of the protein and roughly perpendicular to the AdoMet ligand binding tunnel (Fig. 5, *A* and *B*). Because the Cϵ methyl donor group of AdoMet is situated at the bottom of this funnel-shaped cavity, this presents a plausible binding site of the consensus TPDYFL C-terminal peptides of the PP2A catalytic subunit. The surface of this cavity is formed by residues belonging to four different regions, namely the N terminus of helix αZ of the core MT domain (Fig. 5*B*, *blue*), helix α1 of region I (Fig. 5*B*, *red*), helix α5 of region III (Fig. 5*B*, *green*), and helix α8 of region IV (Fig. 5*B*, *orange*). The tip of the cavity only gives access to the methyl group of the AdoMet moiety. Because of the restricted geometry of the cavity and limited access to the methyl donor, the acceptor substrate needs to penetrate deeply inside the cavity, precluding methylation of residues belonging to a structured protein region.

In PP2A catalytic subunits, the six terminal residues (TPDYFL) are conserved. The crystal structure of the homologous PP1 phosphatase (46% sequence identity to PP2A; Ref. 25) indicates that the C-terminal region, including the six conserved residues, is probably unstructured. This permits the C-terminal leucine to enter deep inside the cavity in proximity to the methyl group on the AdoMet. In Fig. 5*A*, rough modeling of the C-terminal peptide in an extended conformation in the PP2A binding site highlights the fact that six residues is the minimal length required to span the depth of the cavity. The strong conservation of the PP2A C-terminal TPDYFL peptide suggests that it may be engaged in specific interactions with the binding cavity of PPM1. This is further confirmed by the conservation of the residues lining the cavity (Arg-81, Cys-202, Leu-204, Tyr-206, Tyr-231, and Tyr-321) and, in particular, the residues from helix α5 that point to the interior of the cavity (Phe-243, Met-247, Asn-250, Leu-251, and Met-259; highlighted in *red* in Fig. 5*B*).

Flexibility of Region III—In crystal form II, residues 236–258 from region III (containing the helix α5 in crystal form I) are disordered. In crystal form I, the residues from this helix have relatively high temperature factors, also indicating intrinsic flexibility. The position and flexibility of this region suggests that it may move in toward the cavity upon acceptor substrate binding (Fig. 5*A*). Helix α5 is well conserved across the different species, and in crystal form I the best conserved residues have their side chains pointing toward the inside of the cavity (Fig. 5*B*), suggesting that helix α5 may be involved in substrate peptide recognition. The absolutely conserved Asp-241 and Phe-243 of this region interact with the equally conserved His-320 and Tyr-321 from region VI, whereas Arg-255 makes a salt bridge to Asp-11 from region I. These two interactions could act as hooks that effectively lock helix α5 in this position.

Catalytic Mechanism—The structure of PPM1 in the presence of AdoMet enables us to propose a catalytic mechanism. The AdoMet carboxylate group is surrounded by a number of deeply buried charged residues, namely Arg-81, Asp-109, Arg-111, and Glu-201 (Fig. 4*B*). A similar surrounding for AdoMet was observed in the protein L-isoaspartyl-methyltransferase (PIMT) that also catalyzes methyl group transfer to a charged carboxylate group (26). Because AdoMet contains both a charged sulfonium atom and peptidic group, charged side chains will contribute favorably to binding. For catechol *O*-methyltransferase, quantum mechanical simulations have been performed on model systems mimicking the methyl transfer from the sulfur atom of an AdoMet cofactor to the hydroxyl oxygen of the catecholate substrate to assess the role of charged residues in the active site (27). These results suggest that the enzymatic acceleration of the reaction comes from the positioning of the reactants in a conformation that differs from that in solution due to the extra charges present in the active site. The positioning of the substrate in the catechol *O*-methyltransferase catalytic site is mediated by a decrease of electrostatic interactions using a Mg^{2+} ion and the binding of other nonpolar residues (28). Arg-81, conserved in all leucine carboxyl MTs (Fig. 3), forms a salt bridge with the carboxylate group of AdoMet but is also in front of the sulfonium group of the methyl donor at the bottom of the putative peptide binding site. It could therefore play a double role: 1) stabilizing a catalytically competent conformation of the AdoMet substrate; and 2) helping to orient the incoming carboxylate of the peptide substrate for a nucleophilic attack on the sulfur atom. A number of well conserved residues are located near the methionyl group and are likely candidates for further coordination of the substrate. These include a stretch of residues between β4 and αD that are conserved in all leucine carboxyl-methyltransferases and, notably, Tyr-206 and Cys-202, which are at a distance of only 3.8 Å from the methyl-group.

Electrostatic Potential of PPM1—Assembly of the PP2A complex seems to start with the formation of AC heterodimers, which are the substrates for methylation by PPM1. Methylation of the C-terminal residue of the C subunit increases the affinity of the core dimer for some B subunits, leading to the formation of the ABC holoenzyme (8, 9). In their study on PP2A holoenzyme assembly, Strack *et al.* have highlighted the importance of charged residues in the binding of the Bγ subunit to

the A and C subunits (29). These charged residues are clustered on the surface of the Bγ subunit and interact with charged residues on the A subunit surface. Whether charged residues are also involved in the binding of the PP2A core to PPM1 remains to be experimentally tested. PPM1 region IV contains a well conserved negative surface patch with a cluster of residues Asp-309, Glu-310 and Glu-312 (conserved patch on region IV in Fig. 5*B*). The conservation of charged surface residues indicates that these residues may be involved in intermolecular interactions. In crystal form I, these residues are involved in intermolecular interactions with the other monomers. Region IV, which is close to the proposed binding cavity of the C-terminal peptide, may therefore contribute to the interaction with the PP2A core dimer (Fig. 5).

Inactivity of PPM2—Yeast contains a second related gene, PPM2, that has 25% sequence identity with PPM1 but has no detectable methyltransferase activity on PP2A (4). PPM2 contains a C-terminal extension of ~300 residues, and homologous genes can be found in *H. sapiens* and *M. musculus*, making a second leucine carboxyl methyltransferase (LCMT) family. This C-terminal extension could interfere with binding of the PP2A core dimer. From the sequence alignment of PPM2 and PPM1 (Fig. 3), it can be concluded that both families have the same overall fold. PPM2 contains most of the conserved residues involved in AdoMet binding and also presents a putative PP2A binding site in region IV. In the peptide binding cavity most of the residues are also conserved, with the notable exception of Asn-250, Leu-251, and Arg-255 located on helix α5 in region III, which are replaced by His, Phe, and Leu/Asn respectively. Cys-202, a residue close to the catalytic site (Fig. 4*B*), is also mutated. The mutation of these residues in the PPM2 family could lead either to a loss of binding specificity for PP2A, to a decreased efficiency of the methyl transfer catalysis, or to direct PPM2 activity to an unidentified target. These residues could be suggested for mutagenesis.

It has been shown that phosphorylation of the tyrosine located on the conserved TPDYFL C-terminal tail of the PP2A C subunit inhibits the enzyme (30). The peptide binding cavity of PPM1 might not be able to harbor a Tyr(P) group. Phosphorylation of this tyrosine may therefore be a mechanism for modulating the methylation of the C-terminal peptide as well as for directly modulating the binding affinity of the PP2A core dimer to the regulatory B subunits.

Conclusion—The structure of PPM1 is a convincing illustration of how the important methyltransferase superfamily uses structural variations on a common core to introduce different substrate specificities. PPM1, a representative of the methyltransferases acting on proteins, uses unique insertions and additions to the methyltransferase core domain to create a specific PP2A binding site. The biological importance of understanding PP2A methylation is warranted by the many essential functions regulated by PP2A in the cell. The structure of PPM1 also provides the molecular basis to study the involvement of PP2A methylation in tau hyperphosphorylation, neurodegeneration, dementia, and progression into Alzheimer's disease and might help the development of anti-Alzheimer's disease drugs.

Acknowledgment—We acknowledge the staff from the European Synchrotron Radiation Facility beam lines for help with data collection.

REFERENCES

1. Virshup, D. M. (2000) *Curr. Opin. Cell Biol.* **12,** 180–185
2. Mumby, M. (2001) *Science's STKE* http://stke.sciencemag.org/cgi/content/full/sigtrans;2001/79/pe1
3. De Baere, I., Derua, R., Janssens, V., Van Hoof, C., Waelkens, E., Merlevede, W., and Goris, J. (1999) *Biochemistry* **38,** 16539–16547
4. Kalhor, H. R., Luk, K., Ramos, A., Zobel-Thropp, P., and Clarke, S. (2001) *Arch. Biochem. Biophys.* **395,** 239–245
5. Wu, J., Tolstykh, T., Lee, J., Boyd, K., Stock, J. B., and Broach, J. R. (2000) *EMBO J.* **19,** 5672–5681
6. Groves, M. R., Hanlon, N., Turowski, P., Hemmings, B. A., and Barford, D. (1999) *Cell* **96,** 99–110
7. Bryant, J. C., Westphal, R. S., and Wadzinski, B. E. (1999) *Biochem. J.* **339 (Pt 2),** 241–246
8. Tolstykh, T., Lee, J., Vafai, S., and Stock, J. B. (2000) *EMBO J.* **19,** 5682–5691
9. Wei, H., Ashby, D. G., Moreno, C. S., Ogris, E., Yeong, F. M., Corbett, A. H., and Pallas, D. C. (2001) *J. Biol. Chem.* **276,** 1570–1577
10. Zolnierowicz, S. (2000) *Biochem. Pharmacol.* **60,** 1225–1235
11. Janssens, V., and Goris, J. (2001) *Biochem. J.* **353,** 417–439
12. Van Hoof, C., and Goris, J. (2003) *Biochim. Biophys. Acta* **1640,** 97–104
13. Schonthal, A. H. (2001) *Cancer Lett.* **170,** 1–13
14. Vafai, S. B., and Stock, J. B. (2002) *FEBS Lett.* **518,** 1–4
15. Hendrickson, W. A., Horton, J. R., and Lemaster, D. M. (1990) *EMBO J.* **9,** 1665–1672
16. Van Duyne, P., Ray, M. V., Bertelsen, A. H., Jackson-Matthews, D. E., Sturmer, A. M., Merkler, D. J., Consalvo, A. P., Young, S. D., Gilligan, J. P., and Shields, P. P. (1993) *Biotechnology* **11,** 64–70
17. Collaborative Computational Project 4 (1994) *Acta Crystallogr. Sect. D Biol. Crystallogr.* **50,** 760–763
18. Terwilliger, T. C., and Berendzen, J. (1999) *Acta Crystallogr. Sect. D. Biol. Crystallogr.* **55,** 849–861
19. Jones, T. A., Zou, J. H., Cowan, S. W., and Kjeldgaard, M. (1991) *Acta Crystallogr.* Sect. *A* **47,** 110–119
20. Navaza, J. (1994) *Acta Crystallogr. Sect. D. Biol. Crystallogr.* **53,** 157–163
21. Djordjevic, S., and Stock, A. M. (1997) *Structure* **5,** 545–558
22. Schubert, H. L., Blumenthal, R. M., and Cheng, X. (2003) *Trends Biochem. Sci.* **28,** 329–335
23. Martin, J. L., and McMillan, F. M. (2002) *Curr. Opin. Struct. Biol.* **12,** 783–793
24. Schluckebier, G., Kozak, M., Bleimling, N., Weinhold, E., and Saenger, W. (1997) *J. Mol. Biol.* **265,** 56–67
25. Egloff, M. P., Benarroch, D., Selisko, B., Romette, J. L., and Canard, B. (2002) *EMBO J.* **21,** 2757–2768
26. Ryttersgaard, C., Griffith, S. C., Sawaya, M. R., MacLaren, D. C., Clarke, S., and Yeates, T. O. (2002) *J. Biol. Chem.* **277,** 10642–10646
27. Kahn, K., and Bruice, T. C. (2000) *J. Am. Chem. Soc.* **122,** 46–51
28. Kuhn, B., and Kollman, P. A. (2000) *J. Am. Chem. Soc.* **122,** 2586–2596
29. Strack, S., Ruediger, R., Walter, G., Dagda, R. K., Barwacz, C. A., and Cribbs, J. T. (2002) *J. Biol. Chem.* **277,** 20750–20755
30. Chen, J., Martin, B. L., and Brautigan, D. L. (1992) *Science* **257,** 1261–1264
31. Westhead, D. R., Slidel, T. W., Flores, T. P., and Thornton, J. M. (1999) *Protein Sci.* **8,** 897–904
32. Gouet, P., Courcelle, E., Stuart, D. I., and Metoz, F. (1999) *Bioinformatics* **15,** 305–308